JOURNAL OF MATERIALS SCIENCE 39 (2004) 5743–5746

# Crystallization kinetics of $Zr_{60}Al_{15}Ni_{25}$ bulk glassy alloy

Z. J. YAN*
*State Key Lab. of Metal Matrix Composites, School of Materials Science and Engineering, Shanghai Jiao Tong University, Shanghai, 200030, People's Republic of China; Taiyuan Heavy Machinery Institute, Taiyuan, 030024, People's Republic of China*
*E-mail: yanzhijie74@sohu.com*

J. F. LI, S. R. HE, H. H. WANG, Y. H. ZHOU
*State Key Lab. of Metal Matrix Composites, School of Materials Science and Engineering, Shanghai Jiao Tong University, Shanghai, 200030, People's Republic of China*

The crystallization kinetics of $Zr_{60}Al_{15}Ni_{25}$ bulk glassy alloy under isochronal and isothermal conditions has been investigated by differential scanning calorimetry (DSC). The microstructure of as-cast $Zr_{60}Al_{15}Ni_{25}$ bulk glassy alloy is observed by high-resolution electron microscopy (HREM). It is found that there exist nanocrystals with a size of about 7 nm in the glassy matrix, which are not observed in the XRD image. The results of Kissinger analysis show that the effective activation energies for glass transition (457 kJ/mol) and crystallization (345 kJ/mol) are high, indicating that it has large thermal stability against crystallization. The crystallization of $Zr_{60}Al_{15}Ni_{25}$ bulk glassy alloy under isothermal annealing can be modeled by the Johnson-Mehl-Avami equation. The crystallization kinetics parameters show that the isothermal crystallization starts from the growth of the pre-existing nanocrystals and the crystallization process is diffusion-controlled.


## 1. Introduction

Since 1988, a series of multicomponent bulk glassy alloys have been produced [1] and great interest has been paid to this new member of glassy materials. The bulk glassy alloys usually exhibit high thermal stability which provides a large experimentally accessible time and temperature window to investigate, even isothermally, the crystallization behavior in the supercooled liquid region. Zirconium-based bulk glassy alloys have great glass forming ability and can be synthesized by conventional casting method, such as suction casting in a copper mold [2–4]. Furthermore, the Zr-based bulk glass formers contain no noble metals, which promises practical application as engineering materials [5]. The crystallization kinetics of bulk glassy alloys is a subject of considerable interest since the properties of these alloys as engineering materials may be significantly changed due to crystallization. In this paper, the crystallization kinetics of $Zr_{60}Al_{15}Ni_{25}$ bulk glassy alloy under isochronal and isothermal annealing conditions is investigated by differential scanning calorimetry (DSC).

## 2. Experimental

An ingot with nominal composition $Zr_{60}Al_{15}Ni_{25}$ was prepared by arc melting a mixture of pure Zr (99.9 wt%), Al (99.99 wt%) and Ni (99.9 wt%) metals in a water-cooled copper crucible under titanium-gettered argon atmosphere. To enhance homogeneity, the ingot was repeatedly melted 4 times. A plate-like specimen with a cross-section of $1 \times 10$ mm$^2$ and length of 50 mm was produced by suction casting in a copper mold, and its glassy nature was verified by X-ray diffraction (XRD) using Cu-$K_\alpha$ radiation. The microstructure of as-cast $Zr_{60}Al_{15}Ni_{25}$ alloy was observed using high-resolution electron microscopy (JEM-2010). The crystallization process of the $Zr_{60}Al_{15}Ni_{25}$ bulk glassy alloy was characterized by differential scanning calorimetry (DSC, NETZCH, DSC 404) under flowing high purity argon. In the case of isochronal heating, the DSC plot was recorded at selected heating rates of 10, 20, 30 and 40 K/min. For the isothermal analysis, the glassy samples were first heated at a heating rate of 50 K/min to a preset temperature at 743, 748, 753 and 758 K, and then held for a certain period of time until the completion of crystallization. The $Al_2O_3$ and Al pans were utilized for the isochronal heating and isothermal annealing, respectively.

## 3. Results and discussion

### 3.1. Crystallization under isochronal heating condition

The as-cast $Zr_{60}Al_{15}Ni_{25}$ specimen is verified to be mostly a single glassy phase (Fig. 1). The linear heating DSC plots recorded at selected heating rates 10,

*Author to whom all correspondence should be addressed.

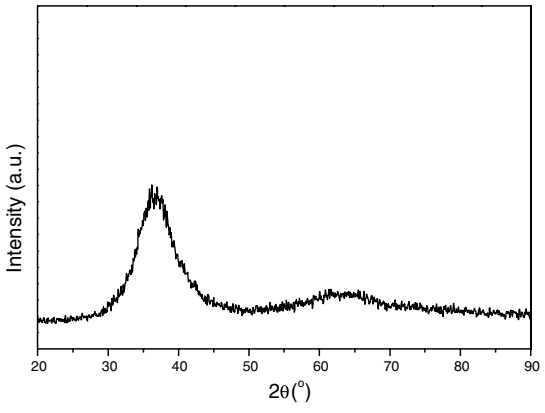


*Figure 1* XRD pattern of a as-cast $Zr_{60}Al_{15}Ni_{25}$ specimen.

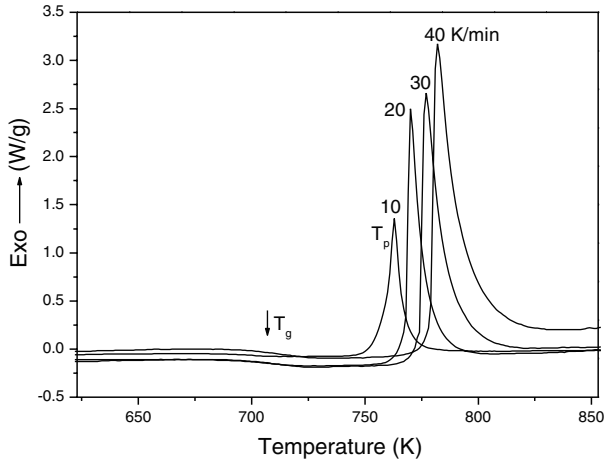


*Figure 2* Isochronal heating DSC plots of as-cast $Zr_{60}Al_{15}Ni_{25}$ alloys at different heating rates.

20, 30 and 40 K/min are shown in Fig. 2. All the DSC traces show an endothermic event, which is the characteristic of glass transition, followed by a single exothermic event corresponding to the crystallization process. The detailed linear heating DSC results are shown in Table I. From the table, it can be seen that the characteristic temperatures $T_g$ and $T_p$ increase as the heating rate increases. The effective activation energies for the glass transition ($E_g$) and crystallization ($E_c$) can be evaluated by Kissinger equation [6]:

$$\ln \frac{T^2}{\beta} = \frac{E}{RT} + \text{Const.} \qquad (1)$$

where $T$ stands for the glass transition temperature $T_g$ or the crystallization peak temperature $T_p$, $\beta$ is the heating rate and $R$ is the gas constant. The Kissinger plots $\ln(T^2/\beta)$ vs. $1/T$ (Fig. 3) are approximately straight lines. Based on the slopes of these Kissinger plots, the

TABLE I Isochronal heating DSC data of as-cast $Zr_{60}Al_{15}Ni_{25}$ alloy at different heating rates

| Heating rate $\beta$ (K/min) | 10 | 20 | 30 | 40 |
|---|---|---|---|---|
| The glass transition temperature $T_g$ (K) | 686.4 | 690.5 | 694.7 | 698.6 |
| The exothermic peak temperature $T_p$ (K) | 763.0 | 770.2 | 777.2 | 781.6 |

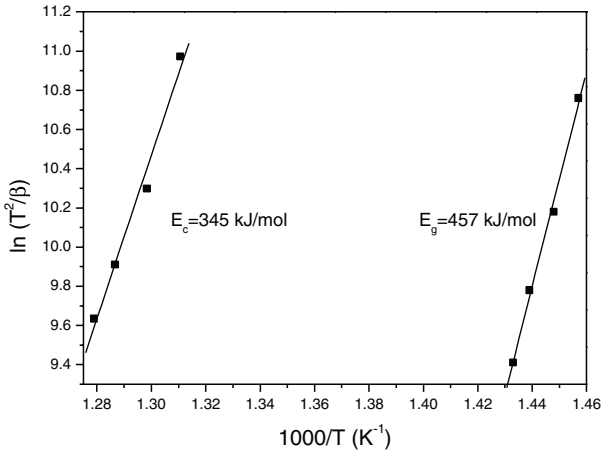


*Figure 3* Kissinger plots of as-cast $Zr_{60}Al_{15}Ni_{25}$ alloy. From whose slopes, the effective activation energies for the glass transition $E_g$ and crystallization $E_c$ are calculated.

effective activation energies $E_g$ and $E_c$ are calculated to be 457 and 345 kJ/mol respectively. These values are much higher than those of $Zr_{41}Ti_{14}Cu_{12.5}Ni_{10}Be_{22.5}$ [7], implying that the $Zr_{60}Al_{15}Ni_{25}$ bulk glassy alloy exhibit higher thermal stability against crystallization.

The high thermal stability of $Zr_{60}Al_{15}Ni_{25}$ bulk glassy alloy is presumably attributed to its dense atomic configuration. The atomic radius of Zr, Al and Ni is 1.600, 1.431 and 1.246 Å, respectively. The ratios of Zr-Al and Zr-Ni atomic pairs are 1.12 and 1.28, respectively. As a result, the Zr-Al-Ni system with significant atomic size difference forms dense random packed atomic configuration [8]. Furthermore, the heats of mixing for Zr-Al, Zr-Ni and Al-Ni atomic pairs in the Zr-Al-Ni system are −44, −49 and −22 kJ/mol, respectively [9], showing a strong attractive interaction with each other in Zr-Al-Ni system. Mobility of atoms in such atomic configuration is obviously difficult. It is not surprising that the effective energy $E_c$ for crystallization is considerably high. It is worth noting that the critical cooling rates of $Zr_{60}Al_{15}Ni_{25}$ and $Zr_{41}Ti_{14}Cu_{12.5}Ni_{10}Be_{22.5}$ are about 100 K/s [2] and 1 K/s [10], which indicating that the glass forming ability of $Zr_{60}Al_{15}Ni_{25}$ is poorer than $Zr_{41}Ti_{14}Cu_{12.5}Ni_{10}Be_{22.5}$. This indicates that thermal stability against crystallization of a glassy alloy cannot effectively reflect its glass forming ability, which is consistent with the observation reported by Lu *et al.* [11].

## 3.2. Crystallization under isothermal annealing condition

The isothermal crystallization kinetics of $Zr_{60}Al_{15}Ni_{25}$ bulk glassy alloy in the supercooled liquid region at 743, 748, 753 and 758 K was investigated by DSC. All the isothermal DSC traces exhibit a single exothermic peak after a certain incubation period (Fig. 4) and the detailed results are shown in Table II. The HREM image of as-cast $Zr_{60}Al_{15}Ni_{25}$ bulk glassy alloy is shown in Fig. 5, showing that there exist numerous short-range order domains with a size of about 7 nm in the glassy alloy. Within the frame of classical homogeneous nucleation theory, the critical radius of the nucleus formed in an amorphous matrix is estimated to be about 1 nm

TABLE II Kinetic parameters of as-cast $Zr_{60}Al_{15}Ni_{25}$ alloy at different isothermal annealing temperatures

| Annealing temperature (K) | 743 | 748 | 753 | 758 |
|---|---|---|---|---|
| Incubation time, $\tau$ (min) | 0.52 | 0.41 | 0.39 | 0.31 |
| Avrami exponent, $n$ | 1.51 | 2.37 | 3.80 | 3.91 |
| Reaction constant, $k$ ($min^{-1}$) | 0.24 | 0.59 | 0.93 | 1.79 |
| Exothermic peak width, $t_{95\%} - t_{1\%}$ (min) | 7.73 | 2.75 | 1.42 | 0.82 |

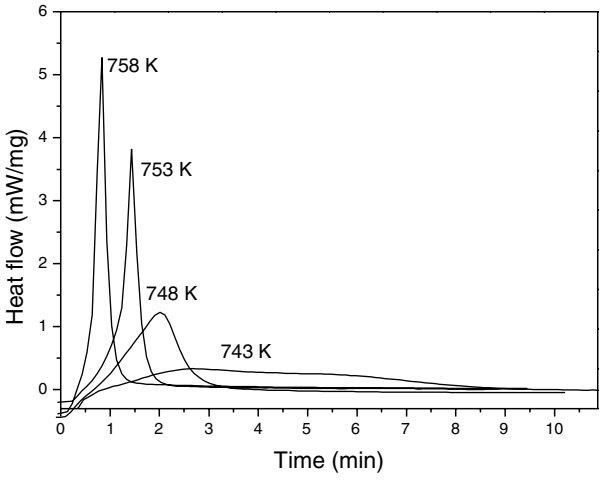


*Figure 4* Isothermal DSC plots of as-cast $Zr_{60}Al_{15}Ni_{25}$ alloy at different annealing temperatures.

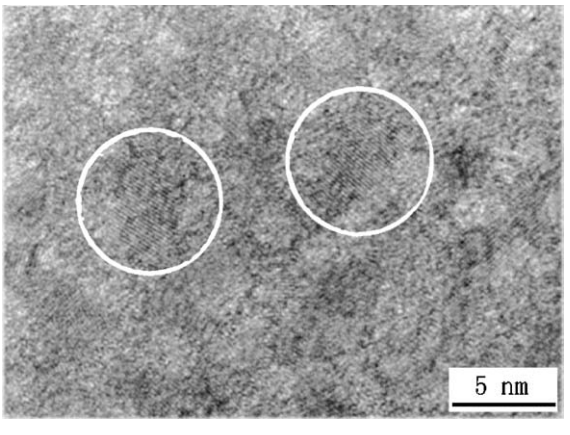


*Figure 5* HREM image of as-cast $Zr_{60}Al_{15}Ni_{25}$ alloy, showing existence of numerous of nanocrystals.

[12]. Hence, the size of these domains in the present $Zr_{60}Al_{15}Ni_{25}$ bulk glassy alloy is overcritical, and therefore, it is more proper to call them nanocrystals. From the Table II, it is clear that the incubation times $\tau$ (defined as the time scale between the time $t_0$ and $t_{1\%}$, $t_0$ is the time to reach the annealing temperature and $t_{1\%}$ the time to reach 1% crystallized volume fraction) for all annealing temperatures are very short and the difference between them is slight, indicating that the crystallization process starts from the growth of pre-existing nanocrystals. The exothermic peak width (referred to the time between 1 and 95% of transformation into the crystalline state) increases as annealing temperature decreases, indicating a sluggish crystallization process.

With the assumption that the crystallized volume fraction $x$, up to any time $t$, is proportional to the partial area of the exothermic peak, the crystallized volume

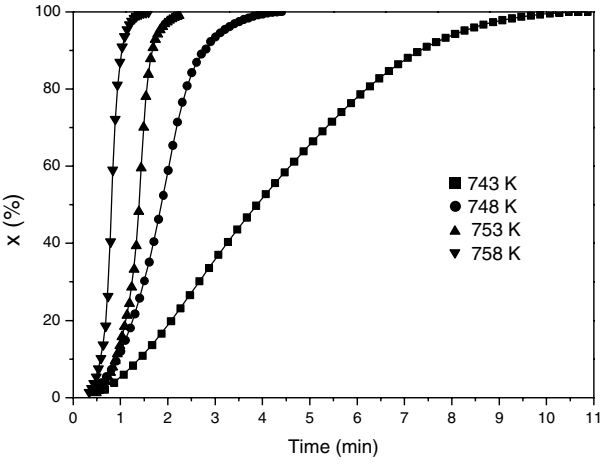


*Figure 6* The crystallized volume fraction as a function of annealing time for as-cast $Zr_{60}Al_{15}Ni_{25}$ alloy at different isothermal temperatures.

fraction corresponding to a given time during crystallization can be determined by measuring the partial area of the exothermic peak. The measured results at different temperatures are shown in Fig. 6. Their shapes are typical sigmoid type. The time evolution of the crystallized volume fraction can be modeled by the Johnson-Mehl-Avrami (JMA) equation as follow [13, 14]:

$$x(t) = 1 - \exp\{-[k(t-\tau)]^n\} \qquad (2)$$

where $x(t)$ is crystallized volume fraction, $t$ the annealing time, $n$, called as Avrami exponent, a constant related to the behavior of nucleation and growth, and $k$ a reaction rate constant.

The double logarithmic form of Equation 2 is expressed as:

$$\ln[-\ln(1-x)] = n\ln k + n\ln(t-\tau) \qquad (3)$$

The JMA plots can be obtained by Plotting $\ln[-\ln(1-x)]$ vs. $\ln(t-\tau)$ at different annealing temperatures for the data $x = 15\%$–$85\%$ (Fig. 7). These plots are nearly straight lines. The Avrami exponent $n$ and the reaction rate constant $k$ can be calculated from the slopes and intercepts of these lines, as shown in Table II. The

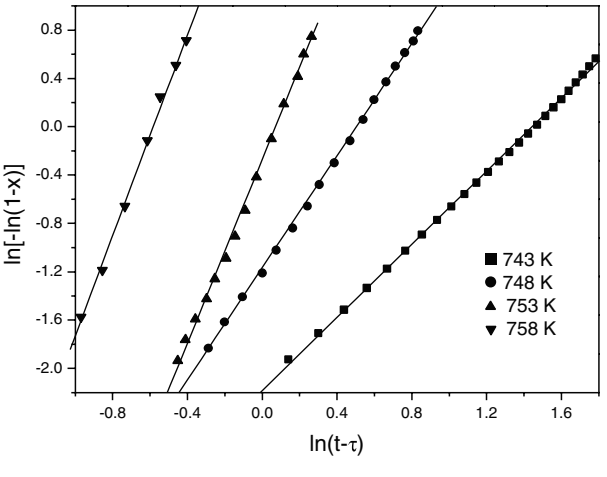


*Figure 7* JMA plots for the crystallization of as-cast $Zr_{60}Al_{15}Ni_{25}$ alloy at different isothermal annealing temperatures.

TABLE III Estimated viscosity of as-cast $Zr_{60}Al_{15}Ni_{25}$ alloy in the supercooled liquid region at different temperatures

| Annealing temperature (K) | 743 | 748 | 753 | 758 |
|---|---|---|---|---|
| Viscosity $\eta$ (Pa s) | $3.15 \times 10^7$ | $2.09 \times 10^7$ | $1.41 \times 10^7$ | $9.63 \times 10^6$ |

large variation of Avrami exponents from 1.5 to 3.9 indicates a change of crystallization mechanism at different isothermal annealing temperatures.

The values of Avrami exponent $n$ (1.5–3.9) indicate that the crystallization of as-cast $Zr_{60}Al_{15}Ni_{25}$ alloy is diffusion-controlled. For the diffusion-controlled crystallization, $1 < n < 1.5$ indicates the growth of particles with an appreciable initial volume; $n = 1.5$, the growth of small particles with a nucleation rate close to zero; $1.5 < n < 2.5$, the growth of small particles with a decreasing nucleation rate; $n = 2.5$, the growth of small particles with a constant nucleation rate; $n > 2.5$, the growth of small particles with an increasing nucleation rate [15]. At 743 K, $n \approx 1.5$, indicating the growth of pre-existing small particles with a nucleation rate close to zero. At 748 K, $1.5 < n < 2.5$, indicating a decreasing nucleation rate with time. At 753 and 758 K, the Avrami exponent is larger than 2.5, implying an increasing nucleation rate.

The diffusion coefficient $D_i$ of component $i$ in a multicomponent system can be expressed as Stokes-Einstein (SE) relation [16]:

$$D_i \propto \eta^{-1} \tag{4}$$

in which $\eta$ is the viscosity. Thus, it is the viscosity that determines the diffusion coefficient $D_i$ which is inversely proportional to the viscosity $\eta$.

It's assumed that the temperature dependence of the viscosity $\eta$ in the supercooled liquid of $Zr_{60}Al_{15}Ni_{25}$ bulk glassy alloy can be expressed by Vogel-Fulcher-Tammann (VFT) relation [17]:

$$\eta = \eta_0 \exp[B/(T - T_0)] \tag{5}$$

where $\eta_0$ and $B$ are constants, $T_0$ corresponds to the VFT temperature which is known to be lower than $T_g$. The effective activation energies $E_g$ and $E_c$ are given by equation as following [18, 19]:

$$E = BRT^2/(T - T_0)^2 \tag{6}$$

where $E$ stands for $E_g$ or $E_c$ and $R$ is the gas constant. The value of $T_0$ is calculated to be 411 K by inserting the values of $E_g$ and $E_c$ (Fig. 3), and the value of $B$ is 9094 (K). Setting $\eta_0$ with $4 \times 10^{-5}$ Pa s [20], the viscosity at different temperatures in the supercooled liquid region can be calculated according to Equation 5, and the detailed results are shown in Table III. From the Table, it is clear that the viscosity of supercooled liquid considerably decreases when the temperature increases. In other words, the diffusion coefficients of atoms increase significantly when the temperature increases, which is the origin of the increase of the nucleation rate as the annealing temperature increases.

## 4. Conclusions

The results of Kissinger analysis show that the effective activation energies for glass transition and crystallization are considerably high, indicating that $Zr_{60}Al_{15}Ni_{25}$ bulk glassy alloy has high thermal stability against crystallization, which is attributed to the dense atomic configuration of Zr-Al-Ni system. The crystallization under isothermal annealing can be modeled by JMA equation. The isothermal crystallization starts from the growth of the pre-existing nanocrystals. From the values of Avrami exponents, it can be known that the crystallization mechanism at different annealing temperatures changes, which is probably attributed to the significant change of the mobility of atoms at different annealing temperatures.

## Acknowledgments

This work was financially supported by the National Natural Science Foundation of China (grant No. 50071032).

## References

1. A. INOUE, *Acta Mater.* **48** (2000) 279.
2. A. INOUE, T. ZHANG and T. MASUMOTO, *Mater. Trans. JIM* **31** (1990) 177.
3. A. INOUE, T. ZHANG, N. NISHIYAMA, K. OHBA and T. MASUMOTO, *ibid.* **34** (1993) 1234.
4. A. PEKER and W. L. JOHNSON, *Appl. Phys. Lett.* **63** (1993) 2342.
5. C. T. LIU, L. HEATHERLY, D. S. EATON, C. A. CARMICHAEL and J. H. SCHNEIBEL, *Metall. Mater. Trans.* A **29A** (1998) 1811.
6. H. E. KISSINGER, *Anal. Chem.* **29** (1957) 1702.
7. Y. X. ZHUANG, W. H. WANG, Y. ZHANG, M. X. PAN and D. Q. ZHAO, *Appl. Phys. Lett.* **75** (1999) 2392.
8. T. ZHANG, A. INOUE and T. MASUMOTO, *Mater. Trans. JIM* **32** (1991) 1005.
9. F. R. DE BOER, R. BOOM, W. C. M. MATTERNS, A. R. MIEDENA and A. K. NIESSEN (eds.), Cohesion in Metals (Elsevier Science, Amsterdam 1989), p. 314.
10. Y. J. KIM. R. BUSCH, W. L. JOHNSON, A. J. RULISON and W. K. RHIM, *Appl. Phys. Lett.* **65** (1994) 2136.
11. Z. P. LU and C. T. LIU, *Acta Mater.* **50** (2002) 3501.
12. M. T. CLAVAGUERA-MORA, N. CLAVAGUERA, D. CRESPO and T. PRADELL, *Prog. Mater. Sci.* **47** (2002) 559.
13. M. A. JOHNSON and R. F. MEHL, *Trans. Am. Inst. Min., Metall. Pet. Eng.* **135** (1939) 416.
14. M. AVRAMI, *J. Chem. Phys.* **9** (1941) 177.
15. J. W. CHRISTIAN (ed.), "Transformation in Metals and Alloys" (Pergamon, 1975) p. 525.
16. A. EINSTEIN (ed.), "Investigation on the Theory of Brownian Motion" (Dover New York, 1956).
17. G. S. FULCHER, *J. Amer Ceram. Soc.* **6** (1925) 339.
18. H. S. CHEN, *Appl. Phys. Lett.* **29** (1976) 12.
19. H. S. CHEN, *J. Non-Cryst. Solids* **27** (1978) 257.
20. S. V. NEMILOV, *Glass Phys. Chem.* **21** (1995) 91.

*Received 31 July 2003*
*and accepted 13 May 2004*